Hadronic transitions $\Upsilon(2S) \to \Upsilon(1S)$

J. P. Alexander, R. Baker, C. Bebek, B. E. Berger, K. Berkelman, K. Bloom, V. Boisvert, D. G. Cassel, D. S. Crowcroft, M. Dickson, S. von Dombrowski, P. S. Drell, K. M. Ecklund, R. Ehrlich, A. D. Foland, P. Gaidarev, R. S. Galik, L. Gibbons, B. Gittelman, S. W. Gray, D. L. Hartill, B. K. Heltsley, P. I. Hopman, J. Kandaswamy, P. C. Kim, D. L. Kreinick, T. Lee, Y. Liu, N. B. Mistry, C. R. Ng, E. Nordberg, M. Ogg,* J. R. Patterson, D. Peterson, D. Riley, A. Soffer, B. Valant-Spaight, and C. Ward
Cornell University, Ithaca, New York 14853

M. Athanas, P. Avery, C. D. Jones, M. Lohner, S. Patton, C. Prescott, J. Yelton, and J. Zheng
University of Florida, Gainesville, Florida 32611

G. Brandenburg, R. A. Briere, A. Ershov, Y. S. Gao, D. Y.-J. Kim, R. Wilson, and H. Yamamoto
Harvard University, Cambridge, Massachusetts 02138

T. E. Browder, Y. Li, and J. L. Rodriguez
University of Hawaii at Manoa, Honolulu, Hawaii 96822

T. Bergfeld, B. I. Eisenstein, J. Ernst, G. E. Gladding, G. D. Gollin, R. M. Hans, E. Johnson, I. Karliner, M. A. Marsh, M. Palmer, M. Selen, and J. J. Thaler
University of Illinois, Urbana-Champaign, Illinois 61801

K. W. Edwards
Carleton University, Ottawa, Ontario, Canada K1S 5B6
and the Institute of Particle Physics, Canada

A. Bellerive, R. Janicek, D. B. MacFarlane, and P. M. Patel
McGill University, Montréal, Québec, Canada H3A 2T8
and the Institute of Particle Physics, Canada

A. J. Sadoff
Ithaca College, Ithaca, New York 14850

R. Ammar, P. Baringer, A. Bean, D. Besson, D. Coppage, C. Darling, R. Davis, S. Kotov, I. Kravchenko, N. Kwak, and L. Zhou
University of Kansas, Lawrence, Kansas 66045

S. Anderson, Y. Kubota, S. J. Lee, J. J. O'Neill, R. Poling, T. Riehle, and A. Smith
University of Minnesota, Minneapolis, Minnesota 55455

M. S. Alam, S. B. Athar, Z. Ling, A. H. Mahmood, S. Timm, and F. Wappler
State University of New York at Albany, Albany, New York 12222

A. Anastassov, J. E. Duboscq, D. Fujino,† K. K. Gan, T. Hart, K. Honscheid, H. Kagan, R. Kass, J. Lee, M. B. Spencer, M. Sung, A. Undrus,‡ R. Wanke, A. Wolf, and M. M. Zoeller
Ohio State University, Columbus, Ohio 43210

B. Nemati, S. J. Richichi, W. R. Ross, H. Severini, and P. Skubic
University of Oklahoma, Norman, Oklahoma 73019

M. Bishai, J. Fast, J. W. Hinson, N. Menon, D. H. Miller, E. I. Shibata, I. P. J. Shipsey, and M. Yurko
Purdue University, West Lafayette, Indiana 47907

S. Glenn, S. D. Johnson, Y. Kwon,§ S. Roberts, and E. H. Thorndike
University of Rochester, Rochester, New York 14627

C. P. Jessop, K. Lingel, H. Marsiske, M. L. Perl, V. Savinov, D. Ugolini, R. Wang, and X. Zhou
Stanford Linear Accelerator Center, Stanford University, Stanford, California 94309

T. E. Coan, V. Fadeyev, I. Korolkov, Y. Maravin, I. Narsky, V. Shelkov, J. Staeck, R. Stroynowski, I. Volobouev, and J. Ye
Southern Methodist University, Dallas, Texas 75275

0556-2821/98/58(5)/052004(15)/$15.00

M. Artuso, F. Azfar, A. Efimov, M. Goldberg, D. He, S. Kopp, G. C. Moneti, R. Mountain, S. Schuh, T. Skwarnicki, S. Stone, G. Viehhauser, and X. Xing
Syracuse University, Syracuse, New York 13244

J. Bartelt, S. E. Csorna, V. Jain,** K. W. McLean, and S. Marka
Vanderbilt University, Nashville, Tennessee 37235

R. Godang, K. Kinoshita, I. C. Lai, P. Pomianowski, and S. Schrenk
Virginia Polytechnic Institute and State University, Blacksburg, Virginia 24061

G. Bonvicini, D. Cinabro, R. Greene, L. P. Perera, and G. J. Zhou
Wayne State University, Detroit, Michigan 48202

M. Chadha, S. Chan, G. Eigen, J. S. Miller, C. O'Grady, M. Schmidtler, J. Urheim, A. J. Weinstein, and F. Würthwein
California Institute of Technology, Pasadena, California 91125

D. W. Bliss, G. Masek, H. P. Paar, S. Prell, and V. Sharma
University of California, San Diego, La Jolla, California 92093

D. M. Asner, J. Gronberg, T. S. Hill, D. J. Lange, R. J. Morrison, H. N. Nelson, T. K. Nelson, D. Roberts, and A. Ryd
University of California, Santa Barbara, California 93106

R. Balest, B. H. Behrens, W. T. Ford, A. Gritsan, H. Park, J. Roy, and J. G. Smith
University of Colorado, Boulder, Colorado 80309-0390

(CLEO Collaboration)

(Received 26 February 1998; published 7 August 1998)

Using a 73.6 pb^{-1} data sample of $\Upsilon(2S)$ events collected with the CLEO II detector at the Cornell Electron Storage Ring, we have investigated the hadronic transitions between the $\Upsilon(2S)$ and the $\Upsilon(1S)$. The dipion transition $\Upsilon(2S)\to\Upsilon(1S)\pi^+\pi^-$ was studied using two different analysis techniques. Selecting events in which $\Upsilon(1S)\to e^+e^-,\mu^+\mu^-$ (''exclusive'' analysis), and using the $\Upsilon(1S)$ leptonic branching fractions world averages from the PDG review, we obtained $\mathcal{B}(\Upsilon(2S)\to\Upsilon(1S)\pi^+\pi^-)=0.189\pm0.004\pm0.010$, while using a method allowing $\Upsilon(1S)\to$anything (''inclusive'' analysis) we obtained $\mathcal{B}(\Upsilon(2S)\to\Upsilon(1S)\pi^+\pi^-)=0.196\pm0.002\pm0.010$. The appropriate weighted average of the two measurements gives $\mathcal{B}(\Upsilon(2S)\to\Upsilon(1S)\pi^+\pi^-)=0.192\pm0.002\pm0.010$. Combining the exclusive and inclusive results we derive the $\Upsilon(1S)$ leptonic branching fractions $\mathcal{B}_{ee}=0.0229\pm0.0008\pm0.0011$ and $\mathcal{B}_{\mu\mu}=0.0249\pm0.0008\pm0.0013$. We also studied $\Upsilon(2S)\to\Upsilon(1S)\pi^0\pi^0$ and obtained $\mathcal{B}(\Upsilon(2S)\to\Upsilon(1S)\pi^0\pi^0)=0.092\pm0.006\pm0.008$. Parameters of the $\pi\pi$ system (dipion invariant mass spectra, angular distributions) were analyzed and found to be consistent with current theoretical models. Lastly, we searched for the η and single π^0 transitions and obtained the 90% confidence level upper limits $\mathcal{B}(\Upsilon(2S)\to\Upsilon(1S)\eta)<0.0028$ and $\mathcal{B}(\Upsilon(2S)\to\Upsilon(1S)\pi^0)<0.0011$. [S0556-2821(98)07417-7]

PACS number(s): 13.20.Gd, 13.25.−k

I. INTRODUCTION

The hadronic transitions in heavy quarkonia provide an experimental testing ground for the theoretical calculations of nonperturbative QCD [1] and can give information on the structure of QCD confinement as well as on the gluon content of light hadrons. Historically, studies of the hadronic transitions $\Upsilon(2S)\to\Upsilon(1S)\pi\pi$ were preceded by investigations of the transitions $\eta'\to\eta\pi\pi$ and $\psi'\to\psi\pi\pi$. All three are examples of $\Delta I=0$ dipion transitions. In the decay $\eta'\to\eta\pi\pi$ the pions fit reasonably well to a phase space mass spectrum [2]. Soon after the discovery of charmonium [3], and the subsequent observation of the $\psi'\to\psi\pi\pi$ transition,

*Permanent address: University of Texas, Austin, TX 78712.
†Permanent address: Lawrence Livermore National Laboratory, Livermore, CA 94551.
‡Permanent address: BINP, RU-630090 Novosibirsk, Russia.
§Permanent address: Yonsei University, Seoul 120-749, Korea.
**Permanent address: Brookhaven National Laboratory, Upton, NY 11973.

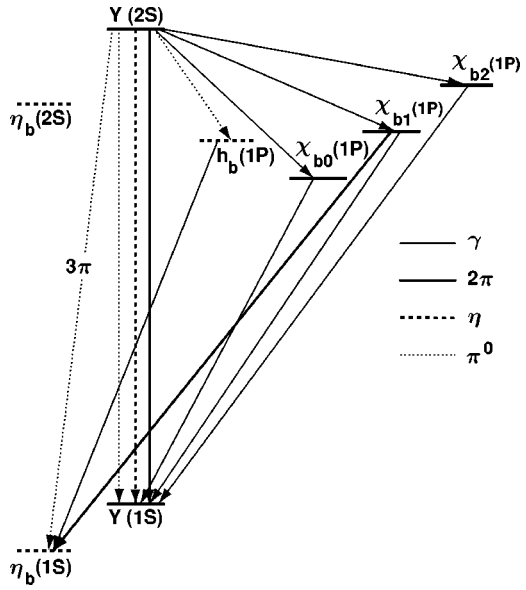

FIG. 1. Transitions in the bottomonium.

it was found that in this transition the dipion invariant mass spectrum cannot be adequately described by a phase space mass spectrum. The challenge of providing an acceptable description of the observed data attracted considerable theoretical attention. With the discovery of another family of heavy quarkonium states, the family of Υ resonances, the theoretical calculations were extended to include bottomonium.

Figure 1 shows the bottomonium levels up to the $\Upsilon(2S)$ and possible transitions between them, including radiative and rare (3π and single π^0) transitions [4]. The hadronic transitions between the bottomonium levels are soft processes (typical transition energies are 0.3–0.9 GeV) and are thereby difficult to treat perturbatively. Typically, the heavy quarkonium hadronic transition $(q\bar{q})'\rightarrow(q\bar{q})X$ is treated as the factorizable product of two processes: first, the transition from $(q\bar{q})'$ to $(q\bar{q})$ with the emission of gluons (usually two), followed by the hadronization of the gluons to the state X (i.e., the production of X from the vacuum in the presence of the gluon color field).

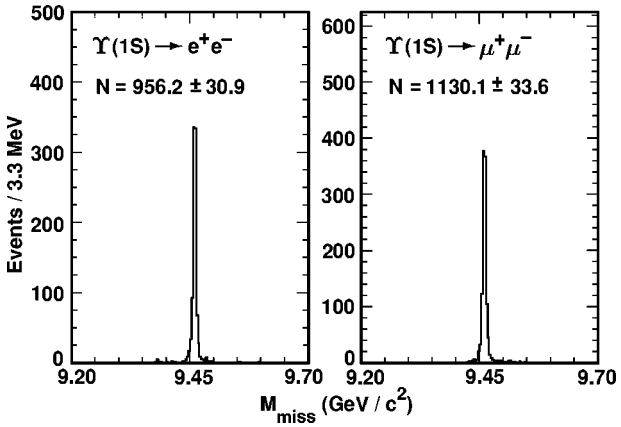

FIG. 2. The missing mass distributions in the exclusive $\Upsilon(2S)\rightarrow\Upsilon(1S)\pi^+\pi^-$ measurement.

TABLE I. Numbers of events observed after background subtraction, efficiencies, product of branching fractions $\mathcal{B}(\Upsilon(2S)\rightarrow\Upsilon(1S)\pi^+\pi^-)\cdot\mathcal{B}(\Upsilon(1S)\rightarrow l^+l^-)$ and branching fraction $\mathcal{B}(\Upsilon(2S)\rightarrow\Upsilon(1S)\pi^+\pi^-)$ for the exclusive measurement.

	$N^{observed}$	ϵ (%)	$\mathcal{B}_{\pi\pi}\cdot\mathcal{B}_{ll}$ ($\times10^{-3}$)	$\mathcal{B}_{\pi\pi}$
ee	956.2 ± 30.9	43.7 ± 1.4	$4.5\pm0.1\pm0.2$	$0.178\pm0.006\pm0.015$
$\mu\mu$	1130.1 ± 33.6	47.5 ± 1.6	$4.9\pm0.1\pm0.2$	$0.196\pm0.006\pm0.011$

Although nonperturbative, the hadronic transitions between heavy quarkonia can nevertheless be described in the context of a ''multipole'' expansion scheme where the gluon fields are expanded in a multipole series, similar to the electromagnetic transitions, as first outlined by Gottfried [5]. In the framework of the multipole expansion, Yan [6], and later Zhou and Kuang [7] calculated the transition rates and derived a parametrization for the dipion invariant mass spectrum in the $\Upsilon(2S)\rightarrow\Upsilon(1S)\pi\pi$ transitions. They used the quark-confining string model [8] to describe the intermediate state of the hadronic transition and calculate the hadronization matrix element. Rather than writing the gluonic degrees of freedom for the quark-confining string, Voloshin and Zakharov [9] (VZ), and afterwards in a revised analysis Novikov and Shifman [10] (NS), used an alternate approach and wrote the general form of the QCD field tensor in the chiral limit to obtain the hadronization matrix element. In both approaches the hadronization matrix element is constrained by current algebra, partial conservation of the axial current (PCAC), and gauge invariance. The essential mass dependence of the matrix element is very similar in all cases: it vanishes for dipion mass approaching threshold, and peaks at larger values of $m_{\pi\pi}$. In the NS and VZ models, the model parameters are derived from ''first-principles,'' as opposed to the Yan *et al.* model where the parameters are determined phenomenologically from a fit to $\psi'\rightarrow\psi\pi\pi$.

The results presented in this paper were obtained using the world's largest available data sample of $\Upsilon(2S)$ decays (73.6 pb^{-1} of integrated luminosity on-resonance, and 5.2 pb^{-1} off-resonance) collected with the CLEO II detector at the Cornell Electron Storage Ring operating at the $\Upsilon(2S)$ center of mass energy in December 1994. Similar investigations were performed by several collaborations including ARGUS [11], CUSB [12], CLEO [13] and Crystal Ball [14]. Our data sample is larger by at least a factor of two in integrated luminosity than each of the previous measurements, with the number of $\Upsilon(2S)$ resonant decays $N_{\Upsilon(2S)}=(488\pm18)\times10^3$ [15].

II. DETECTOR

CLEO II is a general purpose detector [16] for measuring charged and neutral particles in the energy range from $\approx$50 MeV to $\approx$6 GeV. Its three concentric wire drift chambers, covering 95% of the solid angle, detect charged particles and perform particle identification using specific ionization energy loss measurements (dE/dx) in the outer chamber. A superconducting coil provides a magnetic field

TABLE II. $\mathcal{B}(\Upsilon(2S)\to\Upsilon(1S)\pi^+\pi^-)\cdot\mathcal{B}(\Upsilon(1S)\to l^+l^-)$ in units of 10^{-3}.

ARGUS [11]	$4.4\pm0.2\pm0.4$
Crystal Ball [14]	$4.9\pm0.4\pm1.0$
CUSB [12]	$5.4\pm0.3\pm0.4$
CLEO [13]	5.4 ± 0.4
LENA [19]	6.1 ± 2.3
this analysis	$4.66\pm0.10\pm0.23$
average	4.82 ± 0.18

of 1.5 T; for charged particles the system achieves a momentum resolution of $(\delta p/p)^2=(0.0015p)^2+(0.005)^2$, where p is the momentum in GeV/c. A time-of-flight system, just outside the drift chambers, consists of plastic scintillation counters and serves as a primary triggering system; it also provides some particle identification information. Beyond the time-of-flight system, but inside the solenoid, is an electromagnetic calorimeter, consisting of 7800 thallium-doped CsI crystals arranged as two endcaps and a barrel region. The central barrel region of the calorimeter covers 75% of the solid angle and achieves an energy resolution of $\delta E/E(\%)=0.35/E^{0.75}+1.9-0.1E$, where E is the shower energy in GeV. The endcaps of the calorimeter extend the solid angle coverage to about 95% of 4π, although energy resolution is not quite as good as in the barrel. Proportional tracking chambers for muon detection are located in between and outside of the iron slabs that provide the magnetic field flux return.

In our analysis we used a customized version of JETSET [17] program as a Monte Carlo event generator. The simulation of propagation and decay of the final state particles through the CLEO II detector is performed by a GEANT [18] based detector simulation package.

III. TRANSITION $\Upsilon(2S)\to\Upsilon(1S)\pi^+\pi^-$

We studied the dipion transition $\Upsilon(2S)\to\Upsilon(1S)\pi^+\pi^-$ using two different techniques. The first one selects events where the $\pi^+\pi^-$ pair is accompanied by an e^+e^- or $\mu^+\mu^-$

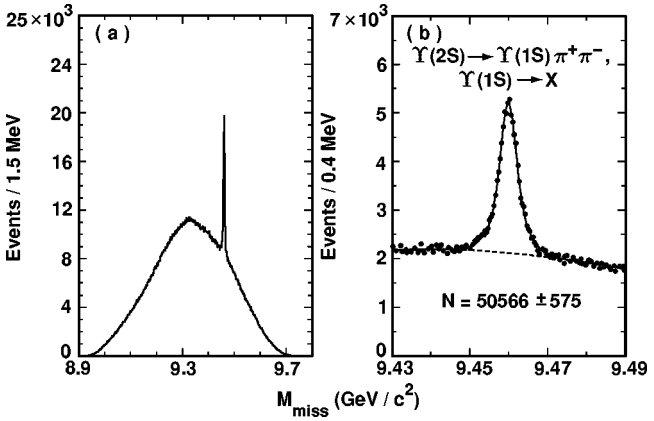

FIG. 3. Missing mass distribution from the inclusive $\Upsilon(2S)\to\Upsilon(1S)\pi^+\pi^-$ events: (a) the full distribution; (b) the region near the $\Upsilon(1S)$ mass, with the fit to the $\Upsilon(1S)$ peak.

TABLE III. $\mathcal{B}(\Upsilon(2S)\to\Upsilon(1S)\pi^+\pi^-)$ inclusive measurements.

LENA [19]	0.26 ± 0.13
ARGUS [11]	$0.181\pm0.005\pm0.010$
CLEO [13]	$0.191\pm0.012\pm0.006$
this analysis	$0.196\pm0.002\pm0.010$[a]
average	0.190 ± 0.007

[a]In the previous CLEO measurement some of the systematic errors were merged into the statistical error.

pair, which is assumed to result from $\Upsilon(1S)\to e^+e^-,\mu^+\mu^-$ (''exclusive'' measurement). In the second technique we select all events which have a $\pi^+\pi^-$ pair (''inclusive'' measurement). The two measurements are complementary to each other and provide us with important cross-checks.

A. Exclusive final states with $\Upsilon(1S)\to e^+e^-,\mu^+\mu^-$

We use the following selection criteria for the exclusive events with $\pi^+\pi^-l^+l^-$ in the final state. We demand four tracks in the event which pass track quality requirements; two of them (the lepton candidate tracks) must have momenta greater than 3.5 GeV/c and originate from a cylindrical volume of transverse dimension 3 mm and longitudinal (along the beam axis) dimension 10 cm centered on the e^+e^- collision point. The other two tracks (the pion candidates) must have momentum less than 0.5 GeV/c and come from a similar cylindrical volume 4 mm×12 cm (radius ×length) centered on the interaction point. To suppress background from radiative Bhabha events with γ conversion we require that the cosine of the angle between the pion tracks satisfy $\cos\theta_{\pi\pi}<0.9$. We identify electrons by the combined requirement that the ratio of the electromagnetic shower energy to the momentum of the matching track is close to 1 and that the lateral energy deposition in the calorimeter is consistent with the electron hypothesis. Events with muons are identified by requiring that the sum of the maximum penetration depths of the two tracks into the muon system absorber be greater than four hadronic absorption lengths.

The missing mass $M_{miss}=\sqrt{(M_{\Upsilon(2S)}-E_{\pi\pi})^2-p_{\pi\pi}^2}$ (i.e., the mass recoiling against the dipion system) distributions for both the ee and $\mu\mu$ channels are shown in Fig. 2. We observe a clean signal with very little background in the side-bands,[1] thus we use a simple event count to obtain the number of observed events both in Monte Carlo (to calculate efficiencies) and in data.

The three largest sources of background are QED radiative processes with γ conversion, two-photon double-tag production of $\pi\pi$ (in the ee channel) and one-prong τ decays from $\Upsilon(1S)\to\tau\tau$. Due to our minimum lepton momentum and lepton identification requirements the contamination

[1]The signal region is defined as the missing mass interval (9.43,9.49) GeV, the side-bands are defined as (9.20,9.40)∪(9.52,9.70) GeV in both dilepton channels.

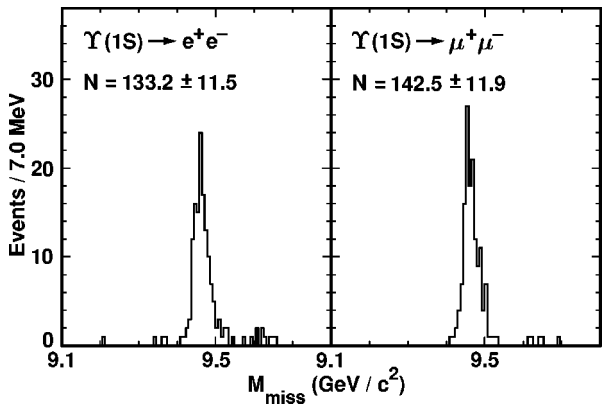

FIG. 4. The missing mass distributions in the exclusive $\Upsilon(2S)\to\Upsilon(1S)\pi^0\pi^0$ measurement.

from τ decays to our data sample (which we directly subtract from the number of observed events) is very small: less than one event in each channel considered. To eliminate QED radiative and two-photon background we use the method of side-band subtraction: we count the number of events in the side-bands of our signal region and extrapolate this number into the signal region. In this way, we find the background contamination to be 8.7 events (0.9%) in the ee channel and 3.8 events (0.3%) in the $\mu\mu$ channel.

Knowing the efficiencies ϵ_{ll} from the Monte Carlo simulation,[2] we can calculate the products of two branching fractions $\mathcal{B}(\Upsilon(2S)\to\Upsilon(1S)\pi^+\pi^-)\cdot\mathcal{B}(\Upsilon(1S)\to l^+l^-) = N_{ll}^{observed}/(\epsilon_{ll}N_{\Upsilon(2S)})$, as shown in Table I. Using the Particle Data Group (PDG) values [20] for $\mathcal{B}(\Upsilon(1S)\to e^+e^-) = 0.0252\pm0.0017$ and $\mathcal{B}(\Upsilon(1S)\to\mu^+\mu^-)=0.0248\pm0.0007$, we determine the $\Upsilon(2S)\to\Upsilon(1S)\pi^+\pi^-$ branching fraction. Combining the results from both channels, we find:

$$\mathcal{B}(\Upsilon(2S)\to\Upsilon(1S)\pi^+\pi^-)=0.189\pm0.004\pm0.010$$

where the first error is statistical and the second is systematic[3] (see Sec. V). In Table II, we compare our result with other exclusive measurements.

B. Inclusive final states with $\Upsilon(1S)\to$anything

In our inclusive analysis of $\Upsilon(2S)\to\Upsilon(1S)\pi^+\pi^-$, $\Upsilon(1S)\to anything$ we select events with at least two tracks ($\pi^+\pi^-$ pair candidates) which pass our track quality requirements, have momentum less than 0.5 GeV/c, come from the interaction region, and satisfy $\cos\theta_{\pi\pi}<0.9$. We also require that the invariant mass of the two pion candidates lie between 0.27 GeV/c^2 and 0.57 GeV/c^2.

The signal appears in the missing mass plot shown in Fig. 3 along with the fit to the $\Upsilon(1S)$ peak. The fitting function we use is a double-Gaussian[4] (with the two Gaussians constrained to the same mean) for the signal, plus a third order polynomial for the background. The number of fitted events in the peak is $N_{incl}=50566\pm575$. The efficiency has been calculated from a Monte Carlo simulation and determined to be $\epsilon_{incl}=(52.9\pm2.0)\%$. From these two numbers and the total number of $\Upsilon(2S)$ produced we find the branching fraction for the transition $\Upsilon(2S)\to\Upsilon(1S)\pi^+\pi^-$:

$$\mathcal{B}(\Upsilon(2S)\to\Upsilon(1S)\pi^+\pi^-) = \frac{N_{incl}}{\epsilon_{incl}N_{\Upsilon(2S)}}=0.196\pm0.002\pm0.010.$$

A comparison of this result with previous inclusive measurements is given in Table III.

Combining the results of the exclusive[5] and inclusive measurements, and taking into account correlations between the systematic errors, we obtain:

$$\mathcal{B}(\Upsilon(2S)\to\Upsilon(1S)\pi^+\pi^-)=0.192\pm0.002\pm0.010.$$

Alternately, knowing the number of observed inclusive and exclusive events, we can solve for the $\Upsilon(1S)$ leptonic branching fractions $\mathcal{B}(\Upsilon(1S)\to l^+l^-)=(N_{ll}\epsilon_{incl})/(N_{incl}\epsilon_{ll})$:

$$B_{ee}=\mathcal{B}(\Upsilon(1S)\to e^+e^-)=0.0229\pm0.0008\pm0.0011$$

$$B_{\mu\mu}=\mathcal{B}(\Upsilon(1S)\to\mu^+\mu^-)=0.0249\pm0.0008\pm0.0013$$

which agree well with the corresponding PDG values.

TABLE IV. Numbers of events observed after background subtraction, efficiencies, product of branching fractions $\mathcal{B}(\Upsilon(2S)\to\Upsilon(1S)\pi^0\pi^0)\cdot\mathcal{B}(\Upsilon(1S)\to l^+l^-)$ and branching fraction $\mathcal{B}(\Upsilon(2S)\to\Upsilon(1S)\pi^0\pi^0)$ for the exclusive measurement.

	$N^{observed}$	ϵ (%)	$\mathcal{B}_{\pi\pi}\cdot\mathcal{B}_{ll}$ ($\times10^{-3}$)	$\mathcal{B}_{\pi\pi}$
ee	133.2 ± 11.5	12.3 ± 1.0	$2.2\pm0.2\pm0.2$	$0.088\pm0.008\pm0.010$
$\mu\mu$	142.5 ± 11.9	12.2 ± 1.0	$2.4\pm0.2\pm0.2$	$0.096\pm0.008\pm0.009$

IV. TRANSITION $\Upsilon(2S)\to\Upsilon(1S)\pi^0\pi^0$

To analyze the transition $\Upsilon(2S)\to\Upsilon(1S)\pi^0\pi^0$ exclusively in the final states with $\Upsilon(1S)\to e^+e^-,\mu^+\mu^-$, we reconstruct the lepton pair using selection criteria identical to those used in our $\Upsilon(2S)\to\Upsilon(1S)\pi^+\pi^-$ exclusive analysis.

We reconstruct π^0 candidates from photon showers in the calorimeter. The photons are required to satisfy the following

[2]For all our sub-analyses we used the Voloshin and Zakharov [9] model with $\lambda=3.44$ to generate the dipion invariant mass spectrum in the Monte Carlo simulation.

[3]When we average over the two dilepton channels, we treat correlated and uncorrelated errors separately in calculating the overall systematic error.

[4]A single Gaussian does not sufficiently accurately parametrize the signal because of the spread in track measuring errors due to different track slope and length, ''hard scatter'' of tracks off the drift chamber material, etc.

[5]Using the 1996 PDG values for the $\Upsilon(1S)$ leptonic branching fractions.

TABLE V. $\mathcal{B}(\Upsilon(2S)\to\Upsilon(1S)\pi^0\pi^0)\cdot\mathcal{B}(\Upsilon(1S)\to l^+l^-)$ in units of 10^{-3}.

ARGUS [11]	$2.3\pm0.4\pm0.5$
Crystal Ball [14]	$2.3\pm0.3\pm0.3$
CUSB [12]	$2.9\pm0.5\pm0.3$
this analysis	$2.29\pm0.14\pm0.20$
average	2.34 ± 0.19

criteria: (1) the absolute value of the cosine of the polar angle (the angle between the photon and the beam axis) should be less than 0.95 to exclude the region of ''hot'' (noisy) crystals in the endcaps close to the beampipe, (2) the photon energy E_γ must lie in the interval $0.05\,\mathrm{GeV}<E_\gamma<0.43\,\mathrm{GeV}$, (3) the angle to the closest projected charged track should be greater than 15°, (4) the shower should not be a fragment of a larger shower, and (5) the pattern of energy deposition should be consistent with the single photon hypothesis. Photons satisfying these requirements are combined into pairs to form π^0 candidates. Combinations with momentum greater than $0.5\,\mathrm{GeV}/c$ are excluded from further consideration. The pair of π^0's remaining with the minimal value of the pull $\sqrt{S^2_{\gamma_1\gamma_2}+S^2_{\gamma_3\gamma_4}}$, where $S_{\gamma\gamma}=(m_{\gamma\gamma}-m_{\pi^0})/\sigma_{m_{\gamma\gamma}}$ is then selected, and the missing mass calculated (Fig. 4). As is the case with charged pions we see clean signals in both lepton channels. Because of the poorer momentum resolution of reconstructed π^0's than that of charged π's, the distributions are considerably wider.

Once again we perform a side-band subtraction[6] to extract the number of observed events (we estimate the background to be 3.8 events, or 2.0%, in the ee channel and 1.4 events, or 1.0%, in the $\mu\mu$ channel).

The yields and efficiencies for exclusive $\Upsilon(2S)\to\Upsilon(1S)\pi^0\pi^0$ transitions are presented in Table IV. From these numbers we calculate the product of branching fractions $\mathcal{B}(\Upsilon(2S)\to\Upsilon(1S)\pi^0\pi^0)\cdot\mathcal{B}(\Upsilon(1S)\to l^+l^-)=N_{ll}^{observed}/(\epsilon_{ll}N_{\Upsilon(2S)})$. Using the PDG values for $\Upsilon(1S)\to l^+l^-$, we determine $\mathcal{B}(\Upsilon(2S)\to\Upsilon(1S)\pi^0\pi^0)$ which is also reported in Table IV. Averaging over the two dilepton channels, we obtain:

$$\mathcal{B}(\Upsilon(2S)\to\Upsilon(1S)\pi^0\pi^0)=0.092\pm0.006\pm0.008.$$

In Table V, previous determinations of $\mathcal{B}(\Upsilon(2S)\to\Upsilon(1S)\pi^0\pi^0)\cdot\mathcal{B}(\Upsilon(1S)\to l^+l^-)$ are compared. From our two exclusive measurements we find the ratio $\mathcal{B}(\Upsilon(2S)\to\Upsilon(1S)\pi^0\pi^0)/\mathcal{B}(\Upsilon(2S)\to\Upsilon(1S)\pi^+\pi^-)=0.49\pm0.06$ which is close to the isospin zero expectation of 0.53.

An inclusive analysis of the $\Upsilon(2S)\to\Upsilon(1S)\pi^0\pi^0$ transition gave a numerically consistent result, however because of the enormous combinatoric background, this measurement has very little statistical weight.

V. TRIGGER EFFICIENCY AND SYSTEMATIC ERRORS

The trigger system of the CLEO II detector, described in detail elsewhere [21], was designed for efficient triggering of two-photon, tau-pair, and hadronic events. There were eight active trigger lines during the $\Upsilon(2S)$ data taking, but only four of them are important in selecting events containing approximately back-to-back electron or muon pairs plus additional energy clusters in the calorimeter. These trigger lines require either two hits in opposite hemispheres in the time-of-flight system or in the calorimeter, or a hit in the time-of-flight barrel region plus a track in the vertex detector (with small variations from line to line). Our estimates of the overall trigger efficiencies from a Monte Carlo simulation of the trigger system are reported in Table VI.

The dominant systematic errors in our analysis come from uncertainties in the total number of produced $\Upsilon(2S)$ resonance events, the leptonic branching fractions of the $\Upsilon(1S)$, and the charged track and π^0 finding efficiency. Other systematic errors are due to uncertainties in trigger efficiencies, event environment effects, the background subtraction, and the shape of the fitting function (inclusive analysis only). The complete breakdown of systematic errors is given in Table VII (relative errors in percent). All these errors are considered to be uncorrelated and separately contribute to the total quoted systematic uncertainties in our branching fractions.

VI. DIPION INVARIANT MASS SPECTRA IN $\Upsilon(2S)\to\Upsilon(1S)\pi\pi$ TRANSITIONS

There have been several theoretical predictions for the dipion invariant mass distribution since a significant difference from phase space was found in $\psi'\to J/\psi\pi\pi$ transitions [22]. As shown in Fig. 5, the dipion transition is treated as a factorizable two-step process: emission of gluons from heavy quarks and the subsequent conversion of the gluons into light hadrons. The dipion invariant mass spectrum is determined by the second step, in the hadronization of the two gluons emitted by the decaying bottomonium—a process which is not well understood.

The following parametrizations were used in fitting our experimental distributions:

Yan [23] model:

TABLE VI. Trigger efficiencies.

	$\Upsilon(2S)\to\Upsilon(1S)\pi^+\pi^-$			$\Upsilon(2S)\to\Upsilon(1S)\pi^0\pi^0$	
	$\Upsilon(1S)\to ee$	$\Upsilon(1S)\to\mu\mu$	$\Upsilon(1S)\to X$	$\Upsilon(1S)\to ee$	$\Upsilon(1S)\to\mu\mu$
Efficiency	0.961 ± 0.008	0.962 ± 0.015	0.990 ± 0.011	0.982 ± 0.031	0.977 ± 0.042

[6]Here the side-bands are (9.10,9.40)∪(9.55,9.80) GeV in both channels and the signal interval is (9.40,9.55) GeV.

TABLE VII. Sources and magnitudes of systematic errors.

	Systematic error (%)		
	$\Upsilon(2S)\to\Upsilon(1S)\pi^+\pi^-$		$\Upsilon(2S)\to\Upsilon(1S)\pi^0\pi^0$
Source	Exclusive	Inclusive	Exclusive
Multiplicity of event	—	2.0	—
Trigger efficiency	0.9/1.6[a]	1.1	3.1/4.2
Tracking	2.8	2.8	—
π^0-finding	—	—	7.0
Finite MC sample	0.5	0.5	0.5
Background subtraction	0.3/0.2	—	1.5/0.9
Leptonic branching fractions	6.7/2.8	—	6.7/2.8
Fitting function	—	0.5	—
$N^{prod}_{\Upsilon(2S)}$	3.7	3.7	3.7
Total	8.2/5.7	5.2	10.9/9.4

[a]separately for $ee/\mu\mu$ channels.

$$\frac{d\sigma}{dm_{\pi\pi}}\propto PS\left[(m^2_{\pi\pi}-2m^2_\pi)^2+\frac{B}{3A}(m^2_{\pi\pi}-2m^2_\pi)\times\left(m^2_{\pi\pi}-4m^2_\pi+2K^2\left(1+\frac{2m^2_\pi}{m^2_{\pi\pi}}\right)\right)+O\left(\frac{B^2}{A^2}\right)\right]$$

where $K=(M_2^2-M_1^2+m^2_{\pi\pi})/2M_2$.

Voloshin and Zakharov [9] model:

$$\frac{d\sigma}{dm_{\pi\pi}}\propto PS\cdot[m^2_{\pi\pi}-\lambda m^2_\pi]^2.$$

Novikov and Shifman [10] model:

$$\frac{d\sigma}{dm_{\pi\pi}}\propto PS\cdot\left[m^2_{\pi\pi}-k(M_2-M_1)^2\left(1+\frac{2m^2_\pi}{m^2_{\pi\pi}}\right)+O(k^2)\right]^2.$$

In all the above formulas $M_2=M_{\Upsilon(2S)}$, $M_1=M_{\Upsilon(1S)}$ and PS is the phase space factor:

$$PS=\sqrt{\frac{(m^2_{\pi\pi}-4m^2_\pi)[M_1^4+M_2^4+m^4_{\pi\pi}-2(M_1^2m^2_{\pi\pi}+M_2^2m^2_{\pi\pi}+M_1^2M_2^2)]}{4M_2^2}}.$$

A. The $\pi^+\pi^-$ invariant mass spectrum

We extract a dipion invariant mass spectrum from both the inclusive and exclusive event samples. The dipion invariant mass spectrum from exclusive events is shown in Fig. 6, where we have combined results from both ee and $\mu\mu$ channels. The inclusive dipion invariant mass spectrum is given in Fig. 7. In both figures the fits to the dipion spectra, using the aforementioned parametrizations are also shown; they are all consistent with our data.

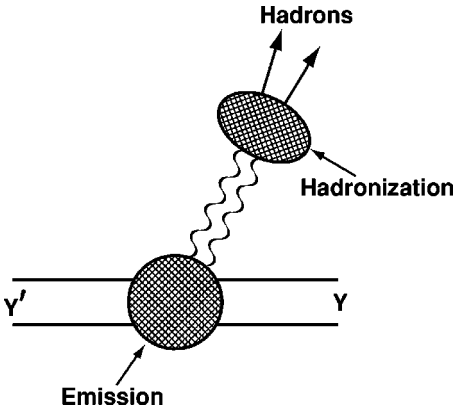

FIG. 5. A hadronic transition as a two-step process.

The data points in the histogram in Fig. 6 are the sideband-subtracted yields for the corresponding bins in $m_{\pi\pi}$, where each data point has been corrected for acceptance (Fig. 8a). To produce the dipion invariant mass spectrum in the inclusive measurement, we use a two-dimensional plot of $m_{\pi\pi}$ vs M_{miss} (shown in Fig. 9) which we slice in bins of $m_{\pi\pi}$, project onto the M_{miss} axis and then fit each projection with a double Gaussian for the $\Upsilon(1S)$ peak plus a third order polynomial to represent the background. We correct the fitted number of $\Upsilon(1S)$ events for

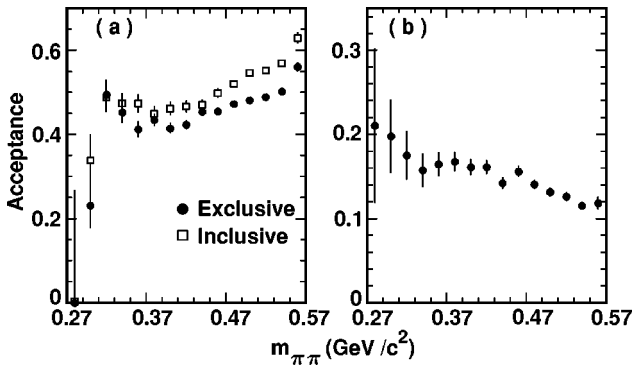

FIG. 6. Dipion invariant mass acceptance for (a) $\Upsilon(2S)\to\Upsilon(1S)\pi^+\pi^-$ and (b) $\Upsilon(2S)\to\Upsilon(1S)\pi^0\pi^0$ events.

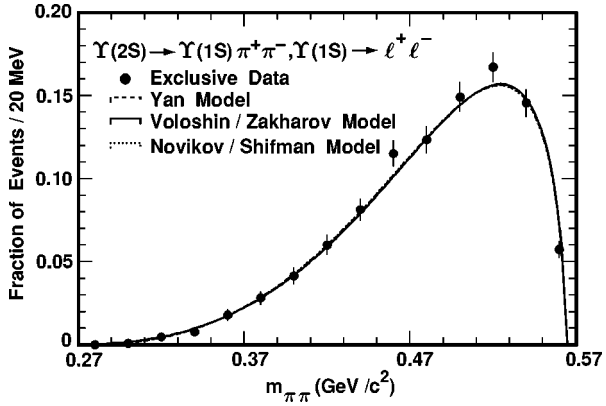

FIG. 7. Dipion invariant mass spectrum from exclusive $\Upsilon(2S) \rightarrow \Upsilon(1S)\pi^+\pi^-$ events (corrected for acceptance).

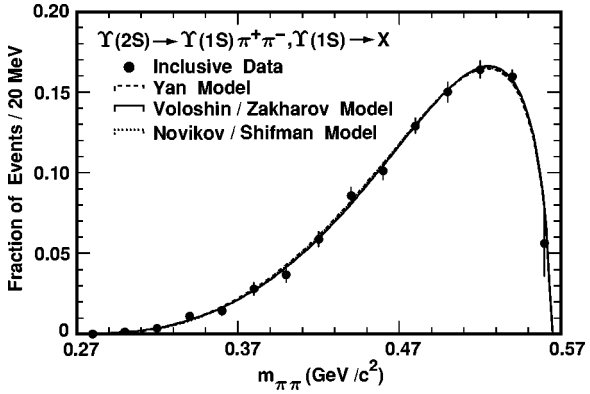

FIG. 9. Dipion invariant mass spectrum from inclusive $\Upsilon(2S) \rightarrow \Upsilon(1S)\pi^+\pi^-$ events (corrected for acceptance).-

acceptance bin-by-bin (Fig. 8a) to obtain the inclusive dipion invariant mass spectrum.

In Table VIII, we have compiled the values of the fitting parameters, their errors, and the χ^2 values of the fits for both the exclusive and inclusive measurements.

B. The $\pi^0\pi^0$ invariant mass spectrum

Similarly to the case of the exclusive $\pi^+\pi^-$ invariant mass spectrum, the $\pi^0\pi^0$ invariant mass spectrum is obtained from the yields of exclusive $\pi^0\pi^0 l^+ l^-$ events in each corresponding $m_{\pi\pi}$ bin, corrected for acceptance (see Fig. 8b). The fits to the acceptance-corrected $\pi^0\pi^0$ invariant mass spectrum are shown in Fig. 10, with fit results reported in Table IX.

C. Combined results for the $\pi\pi$ invariant mass measurements

In order to compare the results of our analysis with the results of other experiments, we perform a simultaneous fit to the exclusive and inclusive $\pi^+\pi^-$ invariant mass spectra. We do not include the $\pi^0\pi^0$ measurement in the combined fit because it has a slightly different parametrization (due to the mass difference between neutral and charged pions) and much lower statistical significance. The fits to the combined data of the exclusive and inclusive $\Upsilon(2S) \rightarrow \Upsilon(1S)\pi^+\pi^-$ decays are shown in Fig. 11. In Table X, we compare the results of our combined fit with the results from previous experiments.

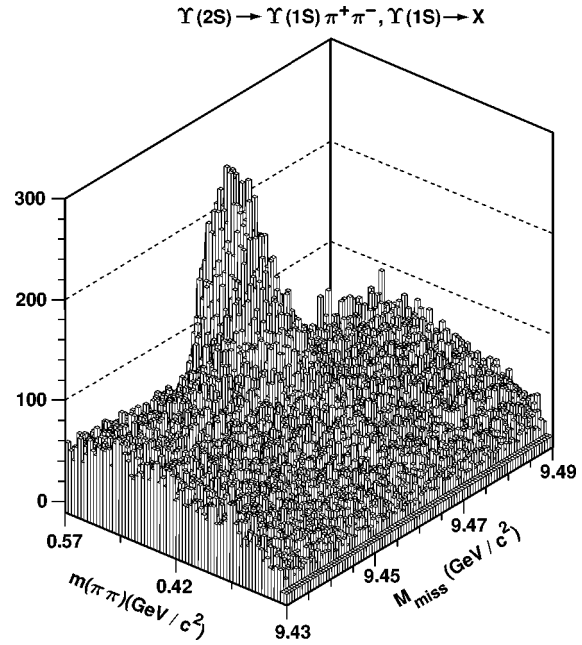

FIG. 8. Dipion invariant mass vs missing mass from the inclusive $\pi^+\pi^-$ events.

VII. ANGULAR DISTRIBUTIONS

The angular distributions in $\pi\pi$ transitions were studied using our exclusive and inclusive $\pi^+\pi^-$ data samples. In e^+e^- annihilation the $\Upsilon(2S)$ is produced polarized with its spin axis lying along the beam axis. This total angular momentum (and its projection onto the beam axis) must be conserved. There are three possible angular momenta in the final state of the dipion transition (Fig. 12): the total spin **J** of the $\Upsilon(1S)$, the internal orbital angular momentum **l** of the dipion system (the total spin of the dipion system $s=0$) and the orbital angular momentum **L** of the dipion system relative to the $\Upsilon(1S)$ [24].

Since the transition is expected to be dominated by $E1 \cdot E1$ gluon radiation, the angular momentum of the $b\bar{b}$ system is not changed by the dipion decay and the polarization of the parent $\Upsilon(2S)$ should be observed in the subsequent decay of the daughter $\Upsilon(1S)$. This is verified in the $\cos\theta$ and ϕ distributions of the outgoing l^+ with respect to the beam shown in Fig. 13: the expected $(1+\cos^2\theta_l)$ distribution is clearly verified and the azimuthal distribution ϕ_{l^+} is reasonably flat, as expected.[7]

The quantum numbers of both the $\Upsilon(2S)$ and $\Upsilon(1S)$ are $J^{PC}=1^{--}$ and $I^G=0^-$; the dipion system has $I^{GC}=0^{++}$. Parity forces l and L to be both even or both odd. The G-parity for the dipion system[8] is 1 and from the formula

[7]CESR beams are not stored long enough to build up appreciable polarization.

[8]The operation of charge conjugation followed by isospin rotation does not change the state of the dipion system.

TABLE VIII. Fit results for the $\pi^+\pi^-$ invariant mass spectrum parametrizations.

	Exclusive events		Inclusive events	
Model	Fit parameters	χ^2/13DF	Fit parameters	χ^2/13DF
Yan [6]	$B/A=-0.132\pm0.018$	15.6	-0.154 ± 0.014	9.3
Voloshin and Zakharov [9]	$\lambda=3.11\pm0.18$	17.5	3.42 ± 0.16	6.6
Novikov and Shifman [10]	$k=0.138\pm0.009$	15.1	0.153 ± 0.008	8.4

$G=(-1)^{l+s+I}$ with $I=0$, $s=0$, $G=1$ we find that l, hence L, must be even.

All theoretical models describing the dipion invariant mass spectrum predict the pions to be emitted predominantly in an s-wave state ($l=0$), although there exists a prediction for the d-wave contribution ($l=2$) [10] of the order of 1%. The d-wave contribution can be observed in the $\cos\theta_\pi^*$ distribution, with θ_π^* determined as the angle of the π^+ in the $\pi\pi$ center of mass frame with respect to the $\pi\pi$ direction. (See Fig. 14 for definitions of angles.) This is shown in Fig. 15 along with the ϕ_π^* distribution which should be flat. It is possible to fit the $\cos\theta_\pi^*$ distribution for our exclusive data sample to a coherent sum of s- and d-waves; ϵ here represents the size of the d-wave contribution:

$$\frac{dN}{d(\cos\theta_\pi^*)}\propto|\sqrt{1-\epsilon^2}Y_0^0+\epsilon Y_2^0|^2$$

with the fit result: $\epsilon=0.077\pm0.041$. In the inclusive measurement (Fig. 16a) the fit result is: $\epsilon=0.028\pm0.027$. Performing a simultaneous fit to the combined data from the exclusive and inclusive measurements (Fig. 16b) we find:

$$\epsilon=0.042\pm0.022.$$

Our results demonstrate the strong s-wave dominance expected in the dipion transition and show some indication of a d-wave contribution on the order of a few percent. In a similar analysis, ARGUS [11] obtained $\epsilon=0.018^{+0.108}_{-0.009}$.

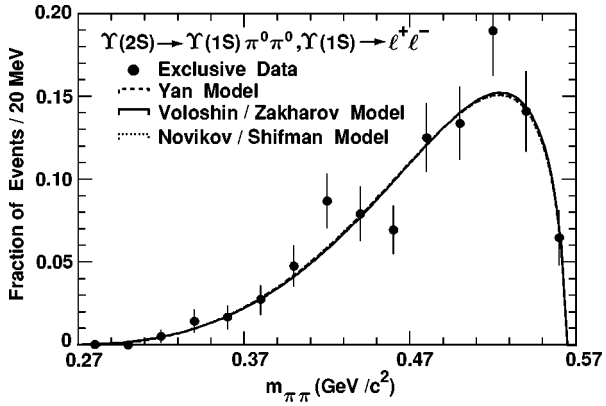

FIG. 10. Dipion invariant mass spectrum from exclusive $\Upsilon(2S)\to\Upsilon(1S)\pi^0\pi^0$ events (corrected for acceptance).

To examine further the question of a possible d-wave contribution we performed a fit to the combined data with the value of ϵ fixed at zero and found the fit confidence level to be 40.2%. Using the χ^2 values from the two combined fits, we performed the F-test[9] for the significance of the d-wave contribution. We calculate $F_\chi=\Delta\chi^2/\chi_n^2=3.5/0.929=3.77$ for $n=21$ DF which means that adding the d-wave to the fitting function significantly improves the fit, alternately, there is a 7% probability that the parent distribution does not have the d-wave term.

The spatial orientation of the $\pi\pi$ system in the e^+e^- frame is consistent with isotropy (Fig. 17) which implies that there is no significant contribution from a ''relative'' D-wave ($L=2$).

VIII. TRANSITION $\Upsilon(2S)\to\Upsilon(1S)\eta$

In our analysis of this transition we used the decay modes where the $\Upsilon(1S)$ decays into a lepton pair (e or μ) and the η decays via one of the modes: $\eta\to3\pi^0\to6\gamma$, $\eta\to2\gamma$, $\eta\to\pi^+\pi^-\pi^0\to\pi^+\pi^-\gamma\gamma$, or $\eta\to\pi^+\pi^-\gamma$ (the total branching fraction of these four modes is 98.2%). The selection criteria common to the four η decay modes are: (1) requirements on the leptonic pair as in our exclusive $\Upsilon(2S)\to\Upsilon(1S)\pi\pi$ analyses, (2) a requirement on the η candidate momentum $p_\eta<0.2$ GeV/c, and (3) a requirement on the dilepton invariant mass 9.21 GeV/$c^2<m_{ll}<9.71$ GeV/c^2.

For the modes $\eta\to3\pi^0\to6\gamma$ and $\eta\to2\gamma$ the following additional criteria are applied: (1) photon requirements as in the exclusive $\Upsilon(2S)\to\Upsilon(1S)\pi^0\pi^0$ analysis except that the energy of γ's from $\eta\to3\pi^0$ must satisfy $E_\gamma<0.33$ GeV and

TABLE IX. Fit results for the $\pi^0\pi^0$ invariant mass spectrum parametrizations.

	Exclusive events	
Model	Fit parameters	χ^2/13DF
Yan [6]	$B/A=-0.145\pm0.040$	10.8
Voloshin and Zakharov [9]	$\lambda=3.35\pm0.49$	11.1
Novikov and Shifman [10]	$k=0.139\pm0.022$	10.9

[9]See, for example, P. R. Bevington, ''Data reduction and error analysis for the physical sciences.''

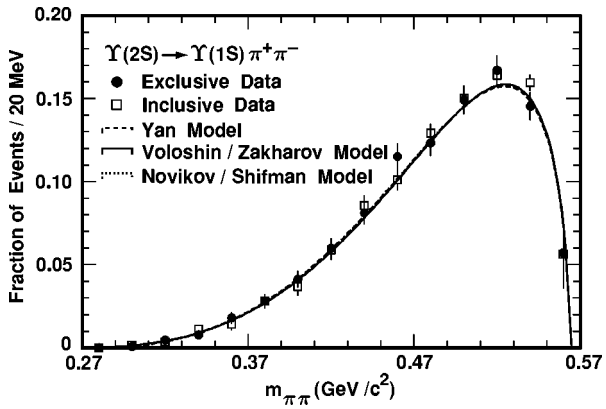

FIG. 11. Combined fit to the dipion invariant mass spectrum from exclusive and inclusive $\Upsilon(2S)\to\Upsilon(1S)\pi^+\pi^-$ events.

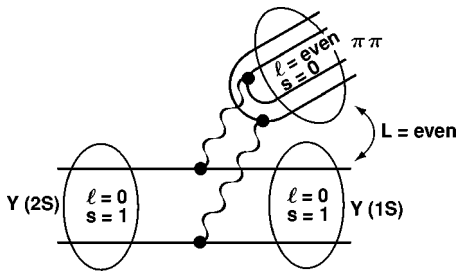

FIG. 12. Angular momenta in the $\pi\pi$ transitions.

those from $\eta\to 2\gamma$ must satisfy $E_\gamma<0.6$ GeV, (2) there should be two good charged tracks in the event, (3) the number of showers in the calorimeter unmatched to charged tracks should be fewer than seven (for $\eta\to 3\pi^0$) or three (for $\eta\to 2\gamma$), (4) for $\eta\to 3\pi^0$ the π^0 candidate momentum must satisfy $p_{\pi^0}<0.3$ GeV/c, and (5) for $\eta\to 2\gamma$ the cosine of the angle between the two photons must satisfy $\cos\theta_{\gamma\gamma}<-0.85$ to reduce the background from the QED process $e^+e^-\to\gamma\gamma e^+e^-$ (since the η's are produced almost at rest, the daughter γ's are close to being back to back).

In the modes $\eta\to\pi^+\pi^-\pi^0\to\pi^+\pi^-\gamma\gamma$ and $\eta\to\pi^+\pi^-\gamma$ we require: (1) the charged pions must pass the same criteria as in the exclusive $\Upsilon(2S)\to\Upsilon(1S)\pi^+\pi^-$ measurement, (2) there must be exactly four good charged tracks in the event, (3) there must be fewer than three (for $\eta\to\pi^+\pi^-\pi^0\to\pi^+\pi^-\gamma\gamma$) or two (for $\eta\to\pi^+\pi^-\gamma$) showers in the calorimeter unmatched to charged tracks, and (4) the cosine of the opening angle between the charged pions must satisfy $\cos\theta_{\pi^+\pi^-}<0.9$ to suppress background from QED processes with gamma conversion $\gamma\to e^+e^-$ where the e^+e^--pair fakes a $\pi^+\pi^-$-pair.

We look for a signal in the scatter plots of the invariant mass of the η candidate vs the missing mass $M_{miss}=\sqrt{(M_{\Upsilon(2S)}-E_\eta)^2-p_\eta^2}$ which are presented in Fig. 18 for the ee channel and in Fig. 19 for the $\mu\mu$ channel (the boxes denote our signal regions which are optimized using a Monte Carlo simulation). In Table XI we list the number of observed events for the decay channels under consideration along with the detection efficiencies of each individual channel as determined from Monte Carlo simulation.

TABLE X. Values of fit parameters using different parametrizations of the $\pi\pi$ invariant mass spectrum.

Model	Yan [6]	Voloshin and Zakharov [9]	Novikov and Shifman [10]
Parameter	B/A	λ	k
Crystal Ball [14]	-0.18 ± 0.15	3.3 ± 1.2	0.14 ± 0.05
CLEO [13]	-0.18 ± 0.06	3.2 ± 0.4	0.15 ± 0.02
ARGUS [11]	-0.154 ± 0.019	3.30 ± 0.19	0.151 ± 0.009
this analysis	-0.145 ± 0.011	3.28 ± 0.12	0.146 ± 0.006

To convert the numbers from Table XI into branching fractions or upper limits we have to consider the sources of possible background contamination. The $\Upsilon(2S)\to\Upsilon(1S)\pi^+\pi^-$ transition with initial or final state radiation can mask the $\Upsilon(2S)\to\Upsilon(1S)\eta$ transition with $\eta\to\pi^+\pi^-\gamma$ and the transition $\Upsilon(2S)\to\Upsilon(1S)\pi^0\pi^0$ where two photons from different π^0's escape detection can mask the η transition with $\eta\to\gamma\gamma$. To estimate these two backgrounds, we subject our Monte Carlo sample of exclusive dipion transitions[10] to the η transition selection criteria. After scaling, we found the background to be 0.2(0.2) events in the $\eta\to\pi^+\pi^-\gamma,ee(\mu\mu)$ channel and 0.3(0.6) events in the $\eta\to\gamma\gamma,ee(\mu\mu)$ channel. We did not observe any background events in the $\eta\to 3\pi^0$ or $\eta\to\pi^+\pi^-\pi^0$ channels. Another possible source of backgrounds are the cascade radiative decays $\Upsilon(2S)\to\gamma\chi_b\to\gamma\gamma\Upsilon(1S)$. This contamination was estimated based on a 15 000 event Monte Carlo sample of the cascade radiative decays. We found no background events from this source. To estimate the background from radiative QED and other possible nonresonant processes we used a data sample corresponding to an integrated luminosity of 5.17 pb^{-1} of e^+e^- annihilations taken at $\sqrt{s}=9.98$ GeV, just below the $\Upsilon(2S)$ resonance. After scaling for luminosity and energy differences we found 14.2(0) background events for the $\eta\to\gamma\gamma$ mode in the $ee(\mu\mu)$ channel and no background events for the three remaining η decay modes. The results of the background study are summarized in Table XII.

Although the above study shows that in the $\mu\mu$ channel the expected number of events from background processes in the signal region is not consistent with the number of observed events, some of the signal events lie very close to the signal box boundary which leads us to interpret our signal candidates as smearing of background events into the signal region. Therefore we (conservatively) do not calculate a branching fraction but set an upper limit. Because the mode $\eta\to\gamma\gamma$ in the ee channel is so ''noisy'' we exclude it from

[10]50 000 events in the $\pi^+\pi^-$ mode and 40 000 events in the $\pi^0\pi^0$ mode.

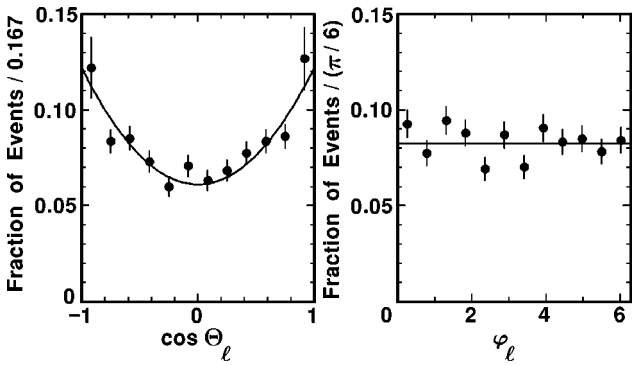

FIG. 13. Angular distributions of l^+ from $\Upsilon(1S)\to l^+l^-$ in the center of mass frame (corrected for acceptance). Solid lines are $dN/d(\cos\theta_l)=N(1+\cos^2\theta_l)$ and $dN/d\phi_l=$const fits.

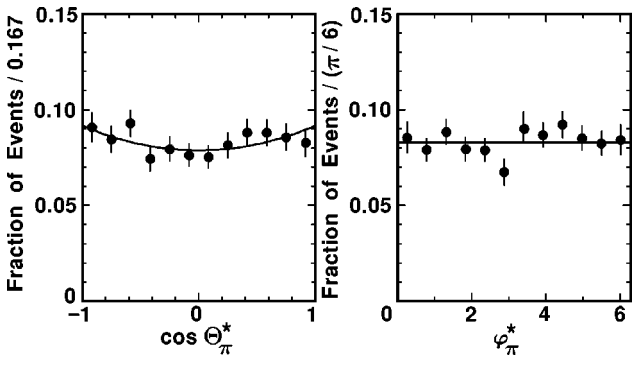

FIG. 15. $\cos\theta_\pi^*$ and ϕ_π^* distributions of π^+ in the center of mass frame of $\pi^+\pi^-$ system in the exclusive $\Upsilon(2S)\to\Upsilon(1S)\pi^+\pi^-$ measurement (corrected for acceptance). Solid lines are $dN/d(\cos\theta_\pi^*)=N|\sqrt{1-\epsilon^2}Y_0^0+\epsilon Y_2^0|^2$ and $dN/d\phi_\pi^*=$const fits.

further analysis. After taking into account the errors on efficiencies, and the errors on the $\Upsilon(1S)$ leptonic and η branching fractions, we set the following upper limit:[11]

$$\mathcal{B}(\Upsilon(2S)\to\Upsilon(1S)\eta)<0.0028(90\%\ \text{C.L.}).$$

The results from other experiments are given in Table XIII.

In the multipole expansion of the gluon color field, $\pi\pi$ transitions proceed via $E1\cdot E1$ emission. The lowest order transition allowed by the quantum numbers of the η-meson is $E1\cdot M2$ or $M1\cdot M1$ emission. This results in a suppression of the η transition compared to the $\pi^+\pi^-$ transition by a factor of $\approx 5\times 10^{-3}$ [28], so the branching fraction for $\Upsilon(2S)\to\Upsilon(1S)\eta$ is expected to be around 0.001, below the current upper limit. Since for the chromomagnetic transitions the transition amplitude varies as m_{quark}^{-4}, the ratio $\mathcal{B}(\Upsilon(2S)\to\Upsilon(1S)\eta)/\mathcal{B}(\Upsilon(2S)\to\Upsilon(1S)\pi^+\pi^-)$ should be substantially smaller than the ratio $\mathcal{B}(\psi(3685)\to\psi\eta)/\mathcal{B}(\psi(3685)\to\psi\pi^+\pi^-)=0.083$. Yan [6] obtained the formula:

$$r_{b/c}=\frac{\Gamma(\Upsilon(2S)\to\Upsilon(1S)\eta)}{\Gamma(\psi(3685)\to\psi\eta)}\simeq\left(\frac{m_c}{m_b}\right)^4\left(\frac{p_\Upsilon}{p_\psi}\right)^3\simeq\frac{1}{275}$$

where p_Υ and p_ψ are the decay momenta. Our experimental value is $r_{b/c}<1/61$, using $\Gamma_{tot}(\psi(3685))=277$ keV and $\mathcal{B}(\psi(3685)\to\psi\eta)=0.027$; this is 15 times smaller than the suppression expected from phase space alone (a factor of four). Our results are clearly consistent with the multipole expansion formalism.

IX. TRANSITION $\Upsilon(2S)\to\Upsilon(1S)\pi^0$

We also studied the isospin violating transition $\Upsilon(2S)\to\Upsilon(1S)\pi^0$ with $\Upsilon(1S)\to l^+l^-$ and $\pi^0\to\gamma\gamma$. The same set

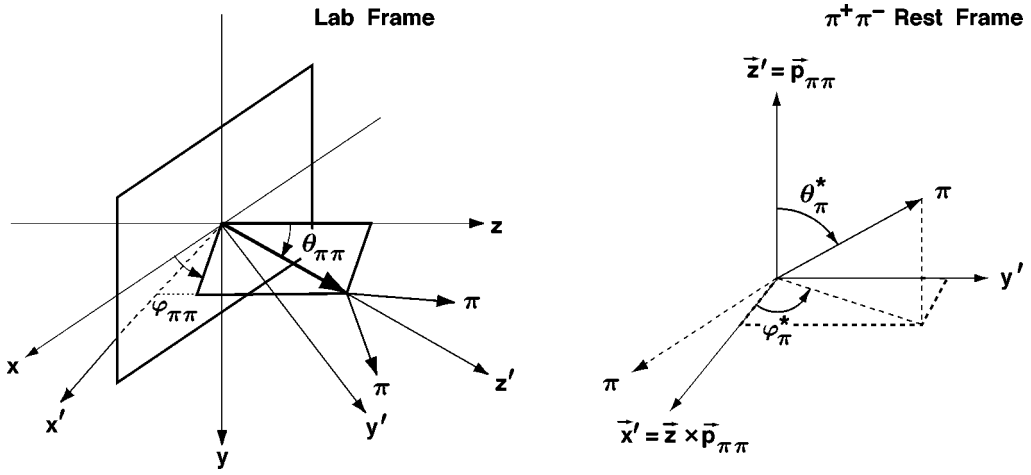

FIG. 14. Frames of reference and definitions of angles for the $\pi\pi$ transitions.

[11]To calculate an upper limit on the number of signal events we follow the procedure suggested by PDG [26] and include the systematic errors according to [27].

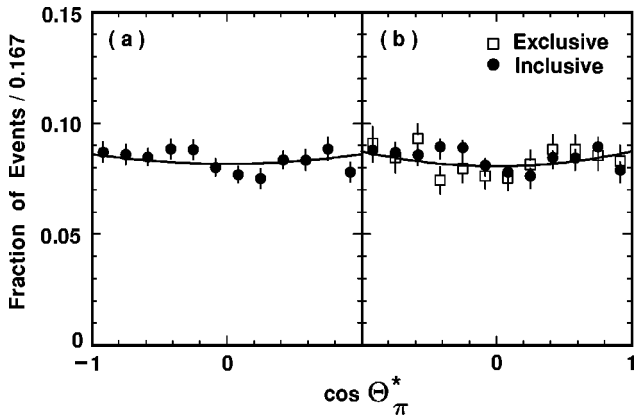

FIG. 16. (a) Fit to the $\cos\theta_\pi^*$ distribution in the inclusive $\Upsilon(2S)\to\Upsilon(1S)\pi^+\pi^-$ measurement. (b) Combined fit to the $\cos\theta_\pi^*$ distributions (corrected for acceptance).

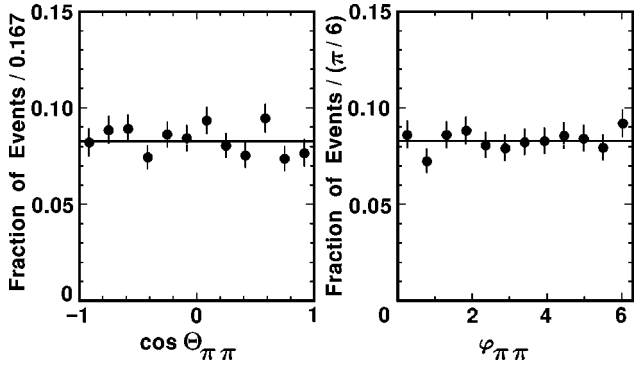

FIG. 17. $\cos\theta$ and ϕ distributions of $\pi^+\pi^-$ system in the e^+e^- frame in the exclusive $\Upsilon(2S)\to\Upsilon(1S)\pi^+\pi^-$ measurement (corrected for acceptance).

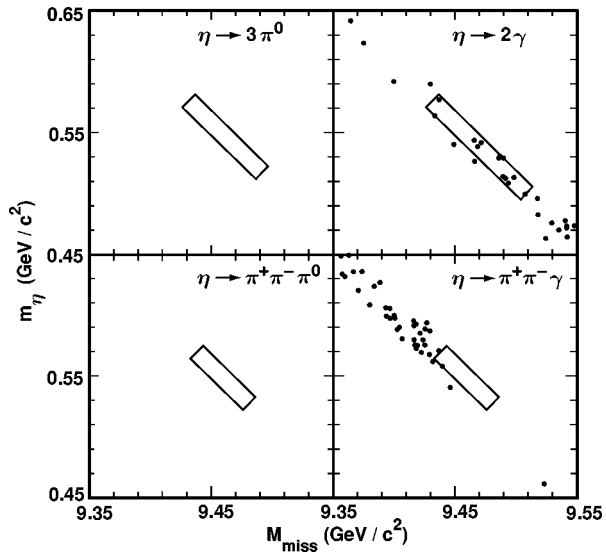

FIG. 18. Signal from $\Upsilon(2S)\to\Upsilon(1S)\eta$, $\Upsilon(1S)\to e^+e^-$ in different η decay modes.

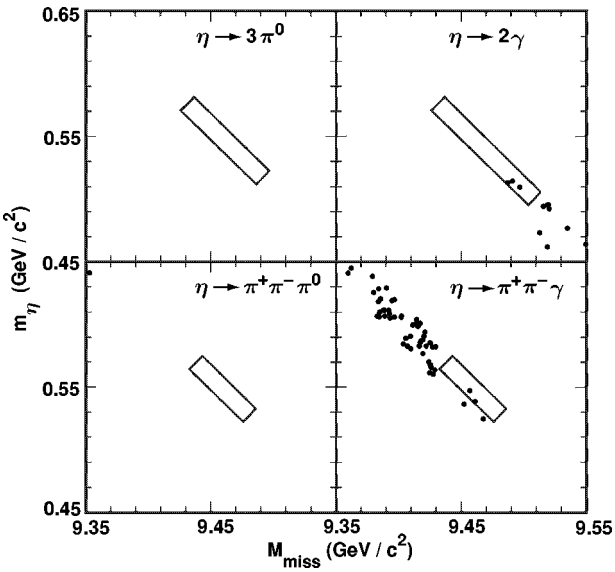

FIG. 19. Signal from $\Upsilon(2S)\to\Upsilon(1S)\eta$, $\Upsilon(1S)\to\mu^+\mu^-$ in different η decay modes.

of selection criteria as in the exclusive $\Upsilon(2S)\to\Upsilon(1S)\pi\pi$ study is applied to lepton candidates and the same set of selection criteria on photons that was used for direct reconstruction of η's from two γ's in the $\Upsilon(2S)\to\Upsilon(1S)\eta$ study is applied here. Additional requirements are: (1) $p_{\pi^0}<0.6$ GeV/c, (2) there must be two good charged tracks, (3) the number of showers unmatched to tracks must be fewer than three, (4) the cosine of the angle between the π^0 and the dilepton system must satisfy $\cos\theta_{\pi ll}<-0.9$ (to reduce the background from QED processes), and (5) $9.21\ \mathrm{GeV}/c^2<m_{ll}<9.71\ \mathrm{GeV}/c^2$ where m_{ll} is the dilepton invariant mass.

As in the search for the η transition, we search for a signal in the scatter plot of the π^0 invariant mass m_{π^0} vs the missing mass $M_{miss}=\sqrt{(M_{\Upsilon(2S)}-E_{\pi^0})^2-p_{\pi^0}^2}$. In Fig. 20 the scatter plots from the $\Upsilon(2S)$ resonance data sample are displayed for both dilepton channels (Monte Carlo simulation is used to optimize the signal regions denoted by the solid boxes).

Within the signal region, we find 9 events in the ee channel and 6 events in the $\mu\mu$ channel. The efficiencies, which

TABLE XI. Numbers of observed events and efficiencies for the $\Upsilon(2S)\to\Upsilon(1S)\eta$, $\Upsilon(1S)\to l^+l^-$ measurement in different η decay modes.

		ee channel		$\mu\mu$ channel	
	Br	$N^{observed}$	Efficiency (%)	$N^{observed}$	Efficiency (%)
$\eta\to 3\pi^0$	0.319	0	2.4±0.3	0	2.3±0.3
$\eta\to 2\gamma$	0.389	13	38.4±1.6	3	46.9±1.9
$\eta\to\pi^+\pi^-\pi^0$	0.236	0	8.9±0.8	0	10.5±0.9
$\eta\to\pi^+\pi^-\gamma$	0.049	1	17.5±2.0	2	22.0±2.2

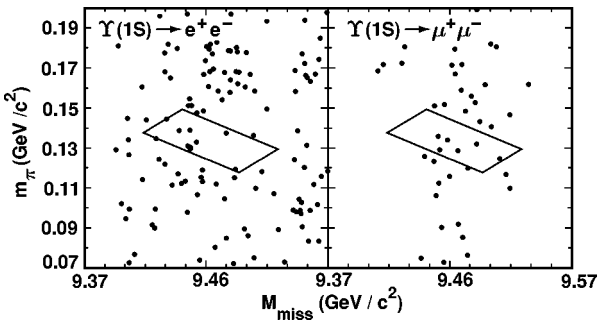

FIG. 20. Scatter plot of π^0 invariant mass vs missing mass for $\Upsilon(2S)\to\Upsilon(1S)\pi^0$, $\Upsilon(1S)\to l^+l^-$ from $\Upsilon(2S)$ resonance data.

are based on Monte Carlo simulation, are given in Table XIV.

We use a ''grand side-band'' technique, to estimate the background: we count the events in the ''grand side-band'' (in Fig. 20 it is the area outside the signal box for the ee channel and a vertical strip between 9.41 GeV and 9.51 GeV in M_{miss}, excluding the signal box, for the $\mu\mu$ channel) and extrapolate the background event yield into the signal region. The results are given in Table XV.

As seen in the table, using the ''grand side-band'' subtraction technique we expect 12.9 background events compared to the total of 15 observed events. This corresponds to an upper limit:

$$\mathcal{B}(\Upsilon(2S)\to\Upsilon(1S)\pi^0)<0.0011(90\%\ \text{C.L.}).$$

This is the most stringent upper limit on the π^0 transition to date. The only other experiment that studied this transition was Crystal Ball (Table XVI).

The $\Upsilon(2S)\to\Upsilon(1S)\pi^0$ transition can occur because of a breaking of the isotopic symmetry due to the mass difference between the u and d quarks, and its rate is expected to be lower than the $\Upsilon(2S)\to\Upsilon(1S)\eta$ rate. In the context of the multipole expansion, this ratio is given by [28]:

$$r_{\pi^0/\eta}\simeq\frac{\Gamma((2S)\to(1S)\pi^0)}{\Gamma((2S)\to(1S)\eta)}=3\left(\frac{m_d-m_u}{m_d+m_u}\right)^2\left(\frac{m_\pi}{m_\eta}\right)^4\left(\frac{p_\pi}{p_\eta}\right)^3.$$

With $(m_d-m_u)/(m_d+m_u)\approx 0.3$ [29] this gives $r_{\pi^0/\eta}\approx 0.022$ for charmonium which is in reasonable agreement with the experimental value of 0.037. For bottomonium we have $r_{\pi^0/\eta}\approx 0.14$ and $\Gamma(\Upsilon(2S)\to\Upsilon(1S)\pi^0)\approx 0.003$ keV (using $\Gamma(\Upsilon(2S)\to\Upsilon(1S)\eta)=0.02$ keV from Kuang-Yan [31]) which is more than an order of magnitude below our upper limit of 0.048 keV.

X. SUMMARY

We have measured various experimental quantities for the hadronic transitions from the $\Upsilon(2S)$ to $\Upsilon(1S)$ including branching fractions, the dipion invariant mass spectra, and angular distributions. Using the PDG value for the full width

TABLE XII. Number of expected background events for the $\Upsilon(2S)\to\Upsilon(1S)\eta$, $\Upsilon(1S)\to l^+l^-$ transition in different η decay modes for our $\Upsilon(2S)$ resonance data sample.

	Sources of background, events in $ee(\mu\mu)$ channel				
Decay mode	$\pi^+\pi^-$	$\pi^0\pi^0$	$\gamma\gamma$ cascade	$\Upsilon(2S)$, continuum	Total
$\eta\to 3\pi^0$	0(0)	0(0)	0(0)	0(0)	0(0)
$\eta\to 2\gamma$	0(0)	0.2(0.2)	0(0)	14.2(0)	14.5(0.2)
$\eta\to\pi^+\pi^-\pi^0$	0(0)	0(0)	0(0)	0(0)	0(0)
$\eta\to\pi^+\pi^-\gamma$	0.3(0.6)	0(0)	0(0)	0(0)	0.3(0.6)

TABLE XIII. Upper limits on $\mathcal{B}(\Upsilon(2S)\to\Upsilon(1S)\eta)$ (90% C.L.).

CLEO [13]	<0.010
Crystal Ball [25]	<0.007
ARGUS [11]	<0.005
CUSB [12]	<0.002
this analysis	<0.0028

TABLE XIV. Number of observed events and efficiencies for the $\Upsilon(2S)\to\Upsilon(1S)\pi^0$, $\Upsilon(1S)\to l^+l^-$ transition.

	$N^{observed}$	Efficiency (%)
ee	9	29.3 ± 0.8
$\mu\mu$	6	36.3 ± 0.9

TABLE XV. Numbers of the events from the ''grand side-band'' subtraction technique.

	$N_{sideband}$	$N_{signal\text{-}region}$	Estimated $N^{background}_{signal\text{-}region}$
ee	130	9	8.4
$\mu\mu$	37	6	4.5

TABLE XVI. Upper limits on $\mathcal{B}(\Upsilon(2S)\to\Upsilon(1S)\pi^0)$ (90% C.L.).

Crystal Ball [25]	<0.008
this analysis	<0.0011

TABLE XVII. Summary of the branching fractions and rates of hadronic transitions of $\Upsilon(2S)$.

	Branching fraction		Rates (keV)	
Decay	Experiment	World Avg.	Experiment	Kuang-Yan
$\Upsilon(2S)\to\Upsilon(1S)\pi^+\pi^-$	$0.192\pm0.002\pm0.010$[a]	0.185 ± 0.008	8.4 ± 0.5	8.8
$\Upsilon(2S)\to\Upsilon(1S)\pi^0\pi^0$	$0.092\pm0.006\pm0.008$	0.088 ± 0.011	4.0 ± 0.4	4.4
$\Upsilon(2S)\to\Upsilon(1S)\eta$	<0.0028	<0.002	<0.12	0.02
$\Upsilon(2S)\to\Upsilon(1S)\pi^0$	<0.0011	<0.008	<0.048	0.003

[a]Average over the exclusive and inclusive measurements.

of the $\Upsilon(2S)$ resonance $\Gamma=44$ keV [30], we also calculate the partial widths for the corresponding transitions. Table XVII reports our measurements of the branching fractions and partial widths compared with previous world averages and theoretical calculations by Kuang and Yan [31]. Our results are consistent with previous experiments as well as theoretical predictions. We determine an upper limit on the branching fraction of $\Upsilon(2S)\to\Upsilon(1S)\eta$ and set a new upper limit on the branching fraction of the $\Upsilon(2S)\to\Upsilon(1S)\pi^0$ transition.

We also calculate the leptonic branching fractions of the $\Upsilon(1S)$: $B_{ee}=\mathcal{B}(\Upsilon(1S)\to e^+e^-)=0.0229\pm0.0008\pm0.0011$ and $B_{\mu\mu}=\mathcal{B}(\Upsilon(1S)\to\mu^+\mu^-)=0.0249\pm0.0008\pm0.0013$ which are in good agreement with PDG values.

The dipion invariant mass spectrum we observe in $\Upsilon(2S)\to\Upsilon(1S)\pi\pi$ transitions is well described by both the Yan model of the gluon color field [7] and the model of Novikov, Shifman, Voloshin and Zakharov who used the general form of the QCD field tensor $G^a_{\mu\nu}$ to obtain a hadronization matrix element in the chiral limit [9,10].

The angular distributions of the final state particles in $\Upsilon(2S)\to\Upsilon(1S)\pi\pi$ show a strong s-wave dominance, as expected from theory. A small d-wave contribution on the order of 4% may be present in our data.

ACKNOWLEDGMENTS

We gratefully acknowledge the effort of the CESR staff in providing us with excellent luminosity and running conditions. J.P.A., J.R.P., and I.P.J.S. thank the NYI program of the NSF, M.S. thanks the PFF program of the NSF, G.E. thanks the Heisenberg Foundation, K.K.G., M.S., H.N.N., T.S., and H.Y. thank the OJI program of DOE, J.R.P., K.H., M.S. and V.S. thank the A.P. Sloan Foundation, R.W. thanks the Alexander von Humboldt Stiftung, M.S. thanks Research Corporation, and S.D. thanks the Swiss National Science Foundation for support. This work was supported by the National Science Foundation, the U.S. Department of Energy, and the Natural Sciences and Engineering Research Council of Canada.

[1] See, e.g., W. Kwong, J. Rosner, and C. Quigg, Annu. Rev. Nucl. Part. Sci. **37**, 325 (1987).
[2] A. Rittenberg, Ph.D. thesis, UCRL, 1969.
[3] G. Abrams *et al.*, Phys. Rev. Lett. **34**, 1181 (1975).
[4] For a review, see M. Voloshin and Yu. Zaitsev, Usp. Fiz. Nauk **152**, 361 (1987) [Sov. Phys. Usp. **30**, 553 (1987)], or D. Besson and T. Skwarnicki, Annu. Rev. Nucl. Part. Sci. **43**, 333 (1993).
[5] K. Gottfried, Phys. Rev. Lett. **40**, 598 (1978).
[6] T.-M. Yan, Phys. Rev. D **22**, 1652 (1980).
[7] H. Y. Zhou and Yu.-P. Kuang, Phys. Rev. D **44**, 756 (1991).
[8] R. Giles and S.-H. Tye, Phys. Rev. D **16**, 1079 (1977).
[9] M. Voloshin and V. Zakharov, Phys. Rev. Lett. **45**, 688 (1980).
[10] V. Novikov and M. Shifman, Z. Phys. C **8**, 43 (1981).
[11] ARGUS Collaboration, H. Albrecht *et al.*, Z. Phys. C **35**, 283 (1987).
[12] CUSB Collaboration, V. Fonseca *et al.*, Nucl. Phys. **B242**, 31 (1984).
[13] CLEO Collaboration, D. Besson *et al.*, Phys. Rev. D **30**, 1433 (1984).
[14] Crystal Ball Collaboration, D. Gelphman *et al.*, Phys. Rev. D **32**, 2893 (1985).
[15] To calculate the total number of $\Upsilon(2S)$ resonant decays, we use the formula $N_{\Upsilon(2S)}=N_{had}/\epsilon_{had}=(N^{on}-N^{off}(L^{on}s^{off}/L^{off}s^{on}))/\epsilon_{had}$, where $N^{on,off}$ is the number of observed hadronic events, $L^{on,off}$ is the integrated luminosity on- and off-resonance, $\sqrt{s}=E_{cm}$, and ϵ_{had} is the probability for any $\Upsilon(2S)$ event to pass our hadronic event selection criteria (based on Monte Carlo calculation).
[16] CLEO Collaboration, Y. Kubota *et al.*, Nucl. Instrum. Methods Phys. Res. A **320**, 66 (1992).
[17] T. Sjostrand, ''PYTHIA 5.7 and JETSET 7.4: Physics and Manual,'' CERN-TH-7112-93 (1994).
[18] R. Brun *et al.*, ''GEANT3 Users Guide,'' CERN DD/EE/84-1 (1987).
[19] LENA Collaboration, B. Niczyporuk *et al.*, Phys. Lett. **100B**, 95 (1981).
[20] Particle Data Group, R. M. Barnett *et al.*, Phys. Rev. D **54**, 1 (1996), p. 548.
[21] C. Bebek *et al.*, Nucl. Instrum. Methods Phys. Res. A **302**, 261 (1991).

[22] T. Himel, Ph.D. thesis, Stanford, 1979.
[23] This particular form is derived from a formula in [6] and explicitly quoted in [13].
[24] R. Cahn, Phys. Rev. D **12**, 3559 (1975).
[25] Crystal Ball Collaboration, B. Lurz *et al.*, Z. Phys. C **36**, 383 (1987).
[26] Particle Data Group [20], p. 166; or O. Helene, Nucl. Instrum. Methods Phys. Res. **212**, 319 (1983).
[27] D. Cousins and V. Highland, Nucl. Instrum. Methods Phys. Res. A **320**, 331 (1992).
[28] M. Voloshin and Yu. Zaitsev, Usp. Fiz. Nauk **152**, 361 (1987) [Sov. Phys. Usp. **30**, 553 (1987)].
[29] J. Gasser and H. Leutwyler, Phys. Rep. **87**, 77 (1982).
[30] Particle Data Group [20], p. 551.
[31] Yu.-P. Kuang and T.-M. Yan, Phys. Rev. D **24**, 2874 (1981).